

2013

# Human injury model for small unmanned aircraft impacts



Civil Aviation Safety Authority  
Civil Aviation Safety Authority /  
Monash University  
12/23/2013

# Revisions

---

<b>Date</b>	<b>Name</b>	<b>Notes</b>
<b>14.10.2013</b>	Alexander Radi	Initial version 0.1
<b>11.11.2013</b>	Alexander Radi	Appendix B added (cutting injuries discussion)
<b>11.11.2013</b>	Alexander Radi	Appendix C added (7kg limit justification)
<b>19.12.2013</b>	Alexander Radi	Abstract rewritten as executive summary
<b>20.12.2013</b>	Alexander Radi	Text streamlined, bibliography added
<b>23.12.2013</b>	Alexander Radi	Grammar corrections

# Executive summary

---

This report describes an injury prediction model for the impact of small Remotely Piloted Aircraft (RPA) into a person on the ground. The model provides estimates of injury severity as a function of the RPA's mass and impact velocity. One of the goals is to determine a 'non-lethal' RPA mass for purpose of drafting air traffic regulations for the rapidly developing civil RPA market.

A literature review of existing injury models from the automotive and defence industries suggested using the Blunt Criterion (BC). This empirical model predicts the severity of blunt trauma injuries (impact without skin penetration) based on the impacting projectile's kinetic energy and impact diameter. In the present study, impacts into the thorax (chest) and head are considered; modifications to the BC for the latter case are discussed. In accordance with other studies, serious injury (AIS=3) is defined as the maximum acceptable injury severity.

The model results indicate a higher sensitivity for head injuries than for injuries to the thorax. The impact into the thorax with a 2kg object at 10m/s (20kts) is survivable with serious injuries. The model predicts the absence of serious head injuries (skull fracture) for an RPA mass under 2kg and impact velocities below 7.5m/s (15kts). In each case a certain minimum 'roundness' of the impacting part is required (at least 10cm impact diameter).

Due to the complex geometry of the RPA and the non-trivial biomechanics of the human body, major simplifications and assumptions had to be made during the adaptation of the BC. The current model ignores the collision dynamics and the RPA material's frangibility and elasticity, making its predictions over-restrictive. On the other hand, certain injury types like brain concussion, heart arrest or neck injury are not considered. Overall, the biggest source of uncertainty results from the application of the BC—which was developed for small projectiles of 20–50mm in diameter and 50–100g mass—to full-scale RPAs.

# 1 Table of Contents

2	Introduction.....	4
2.1	Objectives .....	4
2.2	Background.....	4
2.3	Method.....	4
2.4	Study structure .....	5
3	Physical background .....	6
3.1.1	Perfectly inelastic collision .....	6
4	Existing Injury prediction models.....	8
4.1	The Blunt Criterion.....	9
4.2	Abbreviated Injury Scale (AIS) .....	10
5	Impact into the thorax .....	11
5.1	Effective mass of the thorax.....	11
5.2	Body wall thickness .....	11
5.3	Impact diameter .....	12
5.4	Experimental injury data.....	12
6	Impact into the head.....	13
6.1	Effective mass of the head .....	13
6.2	Wall thickness.....	13
6.3	Impact diameter .....	13
7	Results.....	17
7.1	Expected velocity range.....	17
7.2	Chest impact.....	18
7.3	Head impact .....	20
8	Discussion of the model.....	23
9	Conclusions.....	25
9.1	Summary .....	25
9.2	Recommendations.....	25
10	APPENDIX.....	26
A.	Calculation of the impactor diameter for head impact.....	26
B.	Cutting injuries by rotating blades .....	27
C.	7kg limit justification.....	28
11	Bibliography .....	29

## 2 Introduction

### 2.1 Objectives

This report presents the findings of a study carried out by Alexander Radi M.Sc.<sup>1</sup> during a four months research internship at CASA (Canberra). The aim of the study is to provide the Standards Development branch at CASA with an assessment of injury severity from the impact of small Remotely Piloted Aircraft (RPA) into a person on the ground. Of particular interest are combinations of RPA mass and impact velocity which cause non-severe injuries.

### 2.2 Background

Recent media reports of small RPAs colliding with structures and hitting—or just missing—people on the ground exemplify the potential danger of operating these machines in populated areas.<sup>234</sup> Not every collision results in serious injuries, implying a minimum RPA mass below which the RPA can be considered as harmless (causing non-severe injuries or fatality upon impact). Currently, there are no guide lines on this limit, which can serve as an appropriate cut-off point for prescriptive regulation, whereby less prescriptive industry / professional standards of practice can be adopted.

Currently, CASA imposes operational restrictions on small RPAs weighing more than 100 grams, because it does not have sufficient data on the potential injury that could be caused to people on the ground resulting from a blunt ballistic impact. It is reasonable to assume that the injury potential correlates to the impact kinetic energy, characteristic diameter of RPA's part contacting the body, attitude on impact, and the frangibility of the unmanned airframe. The present study attempts to examine the influence of these parameters on the expected injury potential. Due to the complexity and the time limitation of the project, simplifying assumptions had to be made regarding the impact attitude and frame frangibility.

### 2.3 Method

The review of available literature concentrated on online medical journals, such as:

- *The Journal of Trauma Injury, Infection, and Critical Care*
- *Medicine & Science in Sports & Exercise*
- *Journal of Biomechanics*
- *International Journal of Legal Medicine*
- *Forensic Science International*,

and on journals from the field of automotive crashworthiness:

- *International Journal of Crashworthiness*
- *Stapp Car Crash Journal*
- *Accident Analysis and Prevention*.

The goal of the review was to find suitable and validated human injury criteria and models, which could be adapted to the present task with minimum modifications. The selected model (the 'Blunt

---

<sup>1</sup> Ph.D. candidate Aerospace Engineering at Monash University, Melbourne

<sup>2</sup> <http://www.smh.com.au/nsw/mystery-drone-collides-with-sydney-harbour-bridge-20131004-2uzks.html>

<sup>3</sup> <http://abclocal.go.com/wabc/story?id=9270668>

<sup>4</sup> <http://rt.com/usa/virginia-bull-run-drone-002/>

Criterion') describes blunt trauma injuries from small ballistic projectiles, such as used by law enforcement agencies in non-lethal weapons. This model is based on animal and human cadaver experiments and predicts various levels of injury severity beyond a simple life/death distinction. The deciding advantage of the selected model over other injury criteria (e.g. from the automotive sector) is the use of the projectile's physical properties for injury prediction, instead of the biomechanical response of the body during impact, such as forces or accelerations.

Once a suitable model had been found, it was modified to describe large-object impacts, such as RPAs. For thorax impacts, these modifications were adopted from previous literature; for head impacts, original modifications had to be developed based on geometry and basic physical principles.

The extension of the existing model to large-object impacts made the validation of the results difficult due to the lack of matching experiments. The results are compared against sports accidents (cricket, baseball) and to head injuries during falls on rigid flat surfaces. Limitations of the model due to neglected effects and uncertainties of the input parameters were identified.

## **2.4 Study structure**

The present document shortly discusses the rationale behind the selected model in sections 3 and 4. Sections 5 and 6 contain the mathematical details of the model and the implemented modifications for chest and head impact, respectively. The model results and partial validations are presented in section 7. It is important to consider the limitations of the model which are discussed in section 8. The conclusions of the study and recommendations regarding the design, weight and velocity limits of small RPAs are summarized in section 9.

### 3 Physical background

#### 3.1.1 Perfectly inelastic collision

The underlying assumption of the proposed injury model is the perfectly inelastic collision, as shown in Figure 1. Prior to the impact (situation *I*), the impacting body of mass  $M_1$  moves at velocity  $V_1$  towards the (for the sake of simplicity) stationary body 2 of mass  $M_2$ . After the impact (situation *II*), both objects move as a combined body of mass  $M_1+M_2$  at the resulting velocity  $V_{II}$ . This situation represents a human (or human part, such as the head) of mass  $M_2$  being impacted by an RPA of mass  $M_1$  at velocity  $V_1$ .

Two physical quantities describe this process: The linear momentum  $p$  and the energy  $E$ . Of interest for the injury prediction is the kinetic energy of the impacting object  $E_{kin,I}$ . After the impact, the smaller fraction of this energy exists in form of the kinetic energy of the two combined masses ( $E_{kin,II}$ ), which move now at  $V_{II}$ . The remaining energy has been transformed into deformation energy  $E_{def}$ , deforming the two bodies. Assuming that the impacting RPA structure is rigid, it is the whole of  $E_{def}$  that ‘deforms’ the human body, causing the actual injuries.

As the impactor mass  $M_1$  increases relative to the target mass  $M_2$ , a smaller fraction of the kinetic energy is transformed into deformation energy (although the absolute  $E_{def}$  increases!), and the target body is accelerated to higher velocities (Figure 2). This leads to high accelerations when a comparably small body part (e.g. head) is hit by a heavy object. Even in the absence of external injuries, these high accelerations can result in a brain concussion or neck injuries (think of a soccer ball hitting the head at high velocity). This type of injury will be excluded in the present model. Yet, if energy absorbing materials are used on the RPA, injuries from high accelerations become more likely.

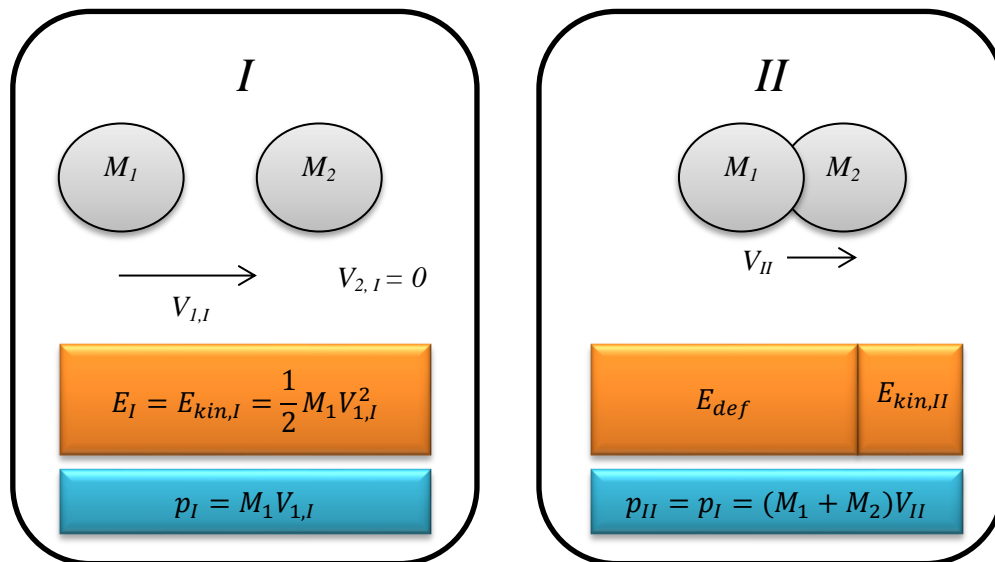


Figure 1: Conservation of energy  $E$  and linear momentum  $p$  in a perfectly inelastic collision.

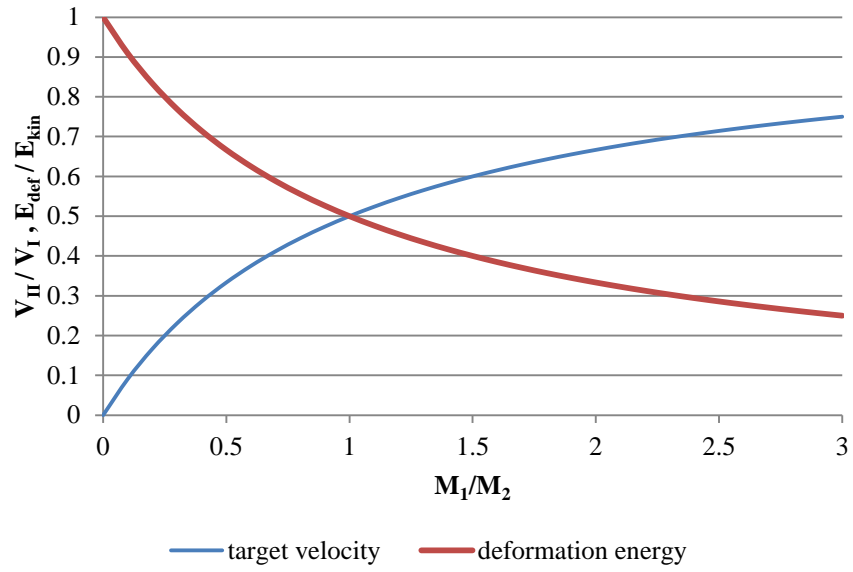


Figure 2: Resulting target velocity and the deformation energy fraction as a function of impactor mass  $M_1$ .

## 4 Existing Injury prediction models

Two industries employ impact injury prediction models: the automotive and the defence industry.

The automotive industry is concerned with predicting and reducing injuries in car, motorbike and pedestrian accidents. Most injuries result from the body, or body parts, impacting other objects, such as dashboards, seats or windscreens (direct interaction). Special cases are injuries due to high accelerations without impact, such as neck injuries ('whiplash'), or fractured ribs due to seatbelt restraint (indirect interaction).

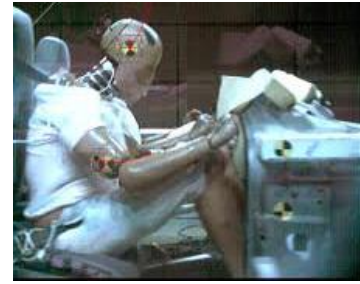


Figure 3: Automotive crash testing

The defence industry deals with inflicting or preventing injuries from high kinetic energy objects, such as projectiles or debris. Within this field, a rather new technology of 'less-lethal kinetic energy munitions' emerged in the last 20–30 years. These munitions are designed to impact the body without producing severe or fatal injuries and are used by law enforcement agencies in riot control.



Figure 4: Russian non-lethal weapon "Wasp"

Although blunt impact injuries (injuries without skin penetration) are important in both fields, the physics involved and the methods of predicting these injuries are quite different. In an automotive crash scenario, the impacting body mass is in the order of 10–100kg, and moves at velocities up to 20m/s (high momentum). A less-lethal projectile weights up to 200g and moves at a maximum velocity of 200m/s. The resulting low momentum leads to extremely short impact durations of 2–5ms and high peak forces (compared to 10–30ms in automotive crashes). The momentum determines the injury biomechanics: crush & shear in the former, and the viscous mechanism in the latter case (Widder, et al., 1997) (Viano, et al., 1992). The velocity and mass of small RPAs reside somewhere between these two scenarios (5–20m/s; 0.5–20kg).

Unfortunately, the methods employed in automotive crash testing make this large pool of data unsuitable for the present study. Figure 5 shows the two different approaches used by the two industries: The automotive industry measures the forces, moments and accelerations of the crash dummy during the impact. These time-resolved measurements are compared to empirical limits to predict the injury severity. These limits were obtained from experiments with animal or human cadavers, in-vivo measurements or by comparison with accident statistics. Such data bases do not exist for RPA impacts, and it is not possible to calculate forces and accelerations from energy or momentum considerations alone.

The less-lethal munitions injury criterion, on the other hand, is directly based on the energy content of the projectile. The link between the energy level and the injury severity is formed by the Blunt Criterion (BC).

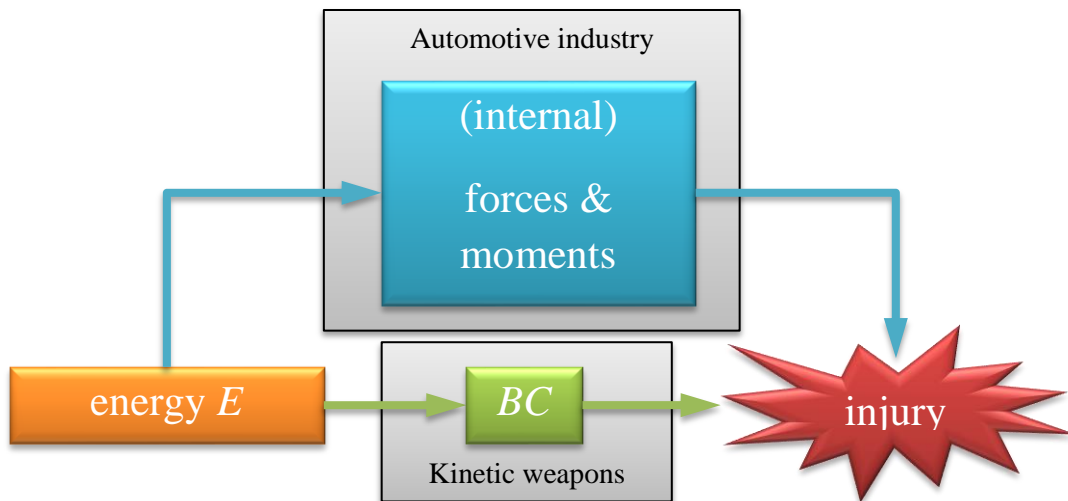


Figure 5: Criteria used to predict the injury severity. The automotive industry relies on measuring the forces and moments in the crash dummy, while the less-lethal kinetic weapons are assessed via the the Blunt Criterion (BC) using the projectile energy  $E$  directly.

#### 4.1 The Blunt Criterion

The BC has been extensively researched for blunt impacts, and is based on research conducted by the U.S. military in the 1970s. This research was commissioned to collect and correlate all existing blunt impact injury data of the thorax (Clare, et al., 1975). The resulting five parameter model is defined as follows (Sturdivan, et al., 2004):

$$BC = \ln \left( \frac{\frac{1}{2}MV^2}{W^{1/3}TD} \right) \quad 1$$

where  $M$ [kg] is the mass,  $V$ [m/s] is the velocity and  $D$ [cm] is the diameter of the projectile,  $W$ [kg] is the mass of the struck body and  $T$ [cm] is the thickness of the body wall. Figure 6 shows the impact situation and parameters.

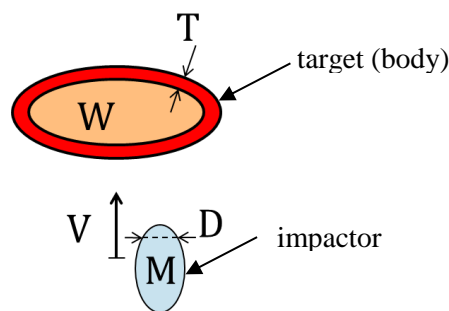


Figure 6: Physical parameters used for the Blunt Criterion.

The BC accounts for the current consensus that the impact energy alone is not an accurate enough predictor of injury. The BC relates the projectile's energy to the capacity of the body to tolerate the inflicted tissue damage. As the equation shows, the numerator represents the kinetic energy of the projectile. The denominator is a semi-empiric expression of the capacity of the body (or body part) to absorb this energy. The scaling takes into account the body mass and the thickness of the protective

wall (ribs, soft tissue) around the vulnerable organs. In addition, the diameter of the projectile provides a scaling for the contact area during the transmission of impact energy.

This criterion was originally developed for chest impacts, and has been extended to head impacts only recently (Raymond, et al., 2009). The present study will use a modified version of this criterion to predict injuries to the thorax and head. Neck injuries will be excluded from the present study as no energy based criterion—equivalent to the BC—exists for this body part, and the results from automotive crash testing are not usable due to reasons discussed above. Furthermore, injuries to the body extremities will be treated as non-life-threatening and thus ignored.

## 4.2 Abbreviated Injury Scale (AIS)

First, a quantitative measure of injury severity needs to be introduced. The Abbreviated Injury Scale (AIS) is one of the most common anatomic scales for traumatic injuries, and is being used internationally. The AIS is an anatomical-based coding system created by the Association for the Advancement of Automotive Medicine to classify and describe the severity of specific individual injuries. It represents the threat to life associated with the injury, rather than the comprehensive assessment of the severity of the injury. The scale ranges from 1 to 6 (Table 1), where 1 is a minor injury, seldom requiring medical treatment, while 6 stands for 100 per cent probability of death. Any injury greater than AIS=3 is considered life-threatening.

<b>AIS code</b>	<b>Injury</b>	<b>Example</b>	<b>AIS % prob. of death</b>
<b>1</b>	Minor	superficial laceration	0
<b>2</b>	Moderate	fractured sternum	1–2
<b>3</b>	Serious	open fracture of humerus	8–10
<b>4</b>	Severe	perforated trachea	5–50
<b>5</b>	Critical	ruptured liver with tissue loss	5–50
<b>6</b>	Maximum	total severance of aorta	100

Table 1: Abbreviated Injury Scale (from [Wikipedia](http://en.wikipedia.org/wiki/Abbreviated_Injury_Scale)<sup>5</sup>)

<sup>5</sup> [http://en.wikipedia.org/wiki/Abbreviated\\_Injury\\_Scale](http://en.wikipedia.org/wiki/Abbreviated_Injury_Scale)

## 5 Impact into the thorax

As seen in Equation 1, the tolerance to blunt impact depends on the human body mass. It is customary to assume 50kg for the 5th percentile female, 75kg for the 50th percentile male and 100kg for the 95th percentile male. In the present study, the injury severity will be calculated for the most vulnerable group, the 5th percentile female with body mass  $W_B = 50\text{kg}$ .

### 5.1 Effective mass of the thorax

In the original formulation of the BC, the mass of projectile was assumed to be much smaller than the body mass. This means that the impact stops the projectile without accelerating the body. Thus, all kinetic energy of the projectile is transformed into deformation energy, which constitutes the numerator in Equation 1. The mass of a small RPA, as considered in the present study, ranges from 0.5–20kg, which is similar or larger than the body part mass (thorax, head). This makes it necessary to consider both, the deformation energy  $E_{def}$  and the remaining kinetic energy in the body/RPA after impact, as shown in Figure 1. As not the whole body is accelerated during impact, *the effective mass*  $W_{BP}$  (Table 2) of the struck body part will be used for the calculation of  $E_{def}$  (Sturdivan, et al., 2004). This is the mass that would move relatively independent of adjacent body parts after an impact by a projectile of comparable mass. The deformation energy is computed as

$$E_{def} = \frac{1}{2} M V^2 \left( 1 - \frac{M}{M + W_{BP}} \right). \quad 2$$

For example, for a  $M=2\text{kg}$  RPA impacting a  $W_B=75\text{kg}$  heavy person at  $V=20\text{m/s}$  in the thorax ( $W_{BP} = 0.21 * W_B$ ), 89 per cent of the total kinetic energy (400J) is inflicted onto the body as deformation energy.

Body Part	Men & Women [%]
Head	N/A
Arm	7
Thorax	21
Midabdomen	21
Pelvis	20
Leg	33

Table 2: Relative body part mass  $W_{BP}$  for injury prediction. (Sturdivan, et al., 2004)

Using Table 2, the effective mass of the thorax will be set to:

$$W_{Th} = 0.21 * 50\text{kg} = 10.5\text{kg} \quad 3$$

### 5.2 Body wall thickness

The body wall thickness  $T$  depends mainly on the body mass. (Sturdivan, et al., 2004) provide the following formula based on laboratory data:

$$T = kW^{1/3}, \quad 4$$

with  $k = 0.59$  for females and  $k = 0.711$  for males. The value for a 50kg female thorax is  $T_{Th} \approx 2.2\text{cm}$ .

### 5.3 Impact diameter

The second modification of the original model consists of an adjustment of the diameter  $D$ . It is the area of contact, represented by  $D$ , which scales the amount of tissue available to absorb the impact energy. When a small, blunt object is involved, the area of contact is just the cross-sectional area of the object. As the size of the object increases, the area of contact is determined by the curvature of the object.

(Sturdivan, et al., 2004) suggested a spherical shape of diameter  $D'$  for simplicity. While impacting, the object pushes into the body, displacing the soft tissue, as seen in Figure 7. If the beginning of injury is considered to be the point at which the sphere has pushed the distance equivalent to the body wall thickness  $T$ , then geometry gives the area of contact  $A$ :

$$A = \pi T(D' - T); \quad D' > 2T. \quad 5$$

The *effective diameter*  $D$  to be used for the thorax in Equation 1 is:

$$D_{Th} = 2\sqrt{A/\pi}. \quad 6$$

It will be assumed that  $D'$  is the local diameter of the RPA part striking the body. Equations 5 and 6 will be used for  $D'$  larger than  $2T_{Th} \approx 5\text{cm}$ .

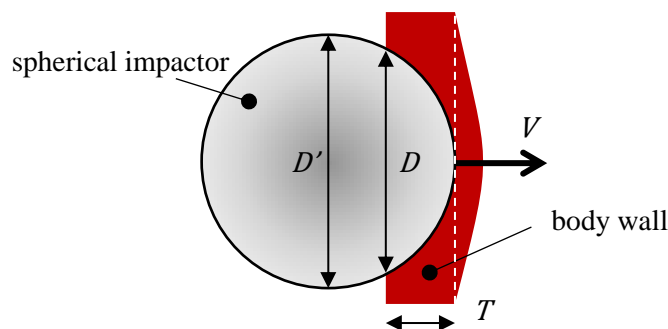


Figure 7: Body wall during impact with a spherical object of diameter  $D' > 2T$ . Note the ‘effective diameter’  $D$ .

### 5.4 Experimental injury data

The BC uses experimental data to relate the deformation energy to injury severity. These data had been obtained by striking animal or human cadaver with impactors and grading the autopsy results according to the AIS. Naturally, the correlation shows a large spread, with particularly large differences between cadaver and in-vivo experiments. For the present study, it is suggested to use the data compiled by (Sturdivan, et al., 2004), who report

$$BC_{Th} = 0.48 \quad 7$$

for a 50 per cent probability of sustaining a serious, but not life threatening AIS=3 injury of the thorax. The probabilities of sustaining other injury severities at BC=0.48 are listed in Table 3.

AIS	1	2	3	4	5	6
probability	86.2%	79.7%	50.0%	16.7%	0.8%	0.1%

Table 3: Probability of injury severity at BC=0.48 based on data from (Sturdivan, et al., 2004).

## 6 Impact into the head

Head injury estimates will be based on the study by (Raymond, et al., 2009), who adopted the BC to the physiology of the skull. The results were derived from experiments consisting of impacting human cadaver heads with ballistic projectiles ( $M = 0.1\text{kg}$ ,  $D = 3.8\text{cm}$ ) at velocities 20 and 35m/s. Skull fracture, which is equivalent to AIS=3 and which leads to a mortality rate of 11 per cent (Raymond, 2008), was defined as the injury criteria. The experiments showed that a 50 per cent risk of skull fracture is represented by

$$BC_H = 1.61. \quad 8$$

This value will be used in the present study as the injury threshold.

The following chapter discusses the necessary adjustments to the parameters in the BC formula (Equation 1), which affect the body wall thickness  $T$ , the body part mass  $W$  and the effective diameter  $D$  (note that (Raymond, et al., 2009) used the head mass as the body part mass as  $W$  in Equation 1).

### 6.1 Effective mass of the head

The post-mortem heads used by Raymond (2009) were detached from the body, such that only absolute head masses were provided (with an average of 3.4kg). The *effective* head mass required for the calculation of  $E_{def}$  can be determined through in-vivo free vibration experiments, as performed by (Lim, 2005):

$$W_H = 6\text{kg}. \quad 9$$

### 6.2 Wall thickness

The body wall thickness  $T$  of the head consists of the skull thickness and the thickness of the surrounding soft tissue. (Raymond, et al., 2009) report a value of

$$T_H = 1.3\text{cm}. \quad 10$$

### 6.3 Impact diameter

The biggest difficulty in adopting the BC to head impacts lies in the determination of the effective diameter  $D$ . For the thorax, the impact geometry consisted of a spherical object hitting a flat surface (chest), which made the determination of  $D$  straightforward. (Raymond, et al., 2009) impacted cadaver heads with flat-faced projectiles, which known diameter could be directly used in Equation 1. In the present study, it must be assumed that the impacting RPA part has a certain curvature defined by its local diameter  $D'$ . The varying local curvature of the head makes the collision geometry even more complex.

As a first simplification, the skull shape will be approximated by a sphere of diameter  $D_{Sk}=18\text{cm}$ . Thus, the geometry under consideration is a spherical impactor depressing a sphere-shaped head to a depth of  $x_{dep}$  (Figure 8).  $D$  is the imprint diameter left in a soft sphere of diameter  $D_H$  after collision with a rigid sphere of diameter  $D'$ . Depending on the experimental conditions and impacting velocities, depression values  $x_{dep}=7-15\text{mm}$  prior to fracture have been reported (Yoganandan & Pintar, 2004). In the present model, the average value from (Raymond, 2008) will be used:

$$x_{dep} = 0.9\text{cm.}$$

The contact diameter (or equivalently the area  $A$ ) between the two spheres will be determined as follows: Based on the idealized skull diameter of  $D_{Sk}=18\text{cm}$ , the range of impactor diameters  $D'$  can be divided into 3 groups:

1.  $T_H < D' \ll D_{Sk}$
2.  $D' \approx D_{Sk}$
3.  $D' \gg D_{Sk}$

The impactor dimensions of the first group are much smaller than the skull size, being in the order of the wall thickness  $T_H$ . The second group consists of impactor sizes comparable to the skull size. And the third group comprises of objects much larger than the head size, with the limiting case of the head hitting a flat surface ('flat plate limit'  $D' \rightarrow \infty$ ).

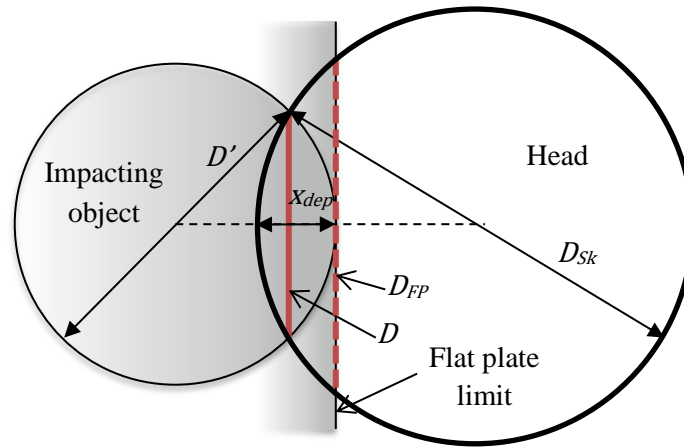


**Figure 8: Impact geometry and dimensions during head impact.**

The impactor size and the depression depth  $x_{dep}$  determine the contact area available for the transmission of the impact energy. It was shown in experiments that different contact areas can result in different fracture mechanisms of the skull (Raymond, 2008). Three failure mechanisms exist, as shown in Figure 9: Small objects with an area less than approximately  $6\text{cm}^2$  ( $<1\text{ inch}^2$ ) are likely to penetrate the skull, leaving a hole of the size of the object itself. Larger impactors break and depress a bone section larger than the impactor area; for this case the BC was validated by (Raymond, et al., 2009). The limiting case of the impact of the head on a flat surface (or a big object) will result in radial propagation of linear fractures through the bone. These three failure modes result from different bone-internal stress responses. Generally, the skull can tolerate larger impact forces for larger contact areas.

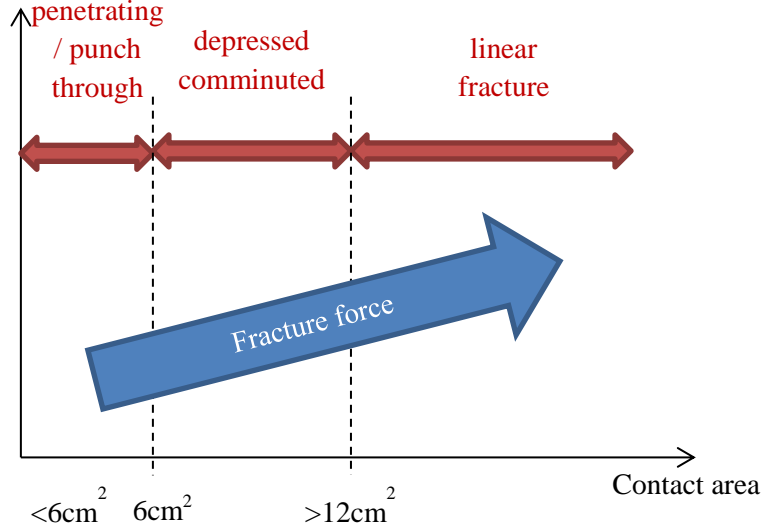


**Figure 9: Different skull failure mechanisms as a function of the contact area between the impactor and head. (Raymond, 2008)**

Not all these scenarios will (and need to) be considered in the present model. At the lower limit, the punch-through case will be ignored, with the assumption that the RPA does not possess sharp protrusions. The existence of such protrusions is likely to lead to skin-penetrating (and skull-penetrating) injuries, which would require a separate injury model.

Mid-sized impactors ( $2T < D' \approx D_{Sk}$ ) will be treated with the BC, extended for spherical impactor shapes. Rearranging Equation 1 gives the effective diameter:

$$D = \frac{E_{def}}{W^{1/3}T_H e^{BC}} = \frac{1}{2} \frac{MV^2}{W^{1/3}T_H e^{BC}} \left(1 - \frac{M}{M + W_H}\right), \quad 12$$

where  $W_H$  is the effective mass of the head,  $W=3.4\text{kg}$  is the head mass used by (Raymond, et al., 2009) and  $M$  and  $V$  are the mass and velocity of the impacting RPA, respectively. Contact diameters larger than  $D$  reduce the risk of fracture by distributing the deformation energy over a larger contact area. Given the contact diameter  $D$  for given impactor mass and velocity (kinetic energy), the minimum allowable impactor diameter  $D'$  can be calculated. Given the depth of the depression  $x_{dep}$ , the impactor diameter is

$$D' = \frac{D^2}{4x_{dep} \left(1 - \frac{D - 2T_H}{D_{FP} - 2T_H}\right)} + x_{dep} \left(1 - \frac{D - 2T_H}{D_{FP} - 2T_H}\right). \quad 13$$

The calculation is based on the radius of a three-point arc, as derived in Appendix A.

Equation 14 already incorporates the upper limit of a large-sized impactor, equivalent to an impact with a flat plate. This case determines the variable  $D_{FP}$ , which is the diameter of the contact area  $A_{FP}$  between a flat surface and a soft sphere depressed by  $x_{dep}$ . Accordingly,  $D'$  goes to infinity when  $D$  approaches  $D_{FP}$ . This means that as the impactor mass and/or velocity increases, the increased deformation energy needs to be distributed over a larger contact area to keep the injury severity constant. The collision geometry imposes an upper limit on the available contact area  $A_{FP}$ , beyond which not even a flat plate provides enough contact surface to spread the energy to prevent injury.

This situation provides a natural limit on the maximum deformation energy, which can be inflicted by a flat-plate impact. This scenario can be used as a ‘cut-off’ point for regulatory purposes, the argument being: “Above this kinetic energy (mass/velocity combination), the probability of a serious head injury (skull fracture) is above the 50 per cent threshold, even if the RPA impacts with one of its flat sides.” When impacting with a curved surface, the tolerable kinetic energy is even lower. The model predicts 76 Joules as the maximum tolerable deformation energy during an impact with a flat surface. The energy density of the contact area is approximately  $1.6\text{J}/\text{cm}^2$ . The validity of these results will be discussed in section 7.3.

## 7 Results

### 7.1 Expected velocity range

The impact velocity plays a dominant role for the prediction of injury severity. The expected velocity values are determined by the impact scenario. (Haddon & Whittaker, 2004) suggest 2 possibilities:

1. *Unpremeditated descent scenario (UDS)*, in which the RPA is under control but unable to maintain altitude, and in which the impact velocity is 30 per cent over minimal (i.e., stall airspeed). The expected velocity range is 10–15m/s for a small RPA.
2. *Loss of control scenario (LCS)*, with the RPA impacting at a velocity 40 per cent higher than maximum airspeed attainable in level flight. The expected velocity lies above 30m/s for small RPAs.

Another scenario is the *uncontrolled descent*, in which the RPA reaches terminal speed based on its drag coefficient (this case is similar to the LCS). (Magister, 2010) showed that this velocity is reached by a small RPA during a descent from an altitude of just 60m AGL, and can be expected to be approximately 30m/s.

Figure 10 exemplifies the high kinetic energies created by these velocities. Although pure kinetic energy has been shown to be not sufficient for accurate injury prediction, rough estimates of expected injury severity based on  $E_{kin}$  are included in this figure (Frank, 2012). Considering energies of 40–120J as dangerous, and >120J as causing severe damage to humans, an impact of a small RPA with a mass of just 0.5kg can be considered as potentially deadly at  $V > 27\text{m/s}$ . The velocities involved in LCS and the terminal velocity scenarios are considerably above the ‘severe damage’ threshold of 120J. For illustration: 120J is equivalent to a mid-size hammer (0.5kg) dropped from the eighth floor (24.5m drop height, 22m/s at impact). Focusing on kinetic energies below 120J, and limiting the RPA mass to 0.5–20kg, the velocity range of interest for the present study becomes 3–22m/s (6–40kts) (marked by the dashed box in Figure 10).

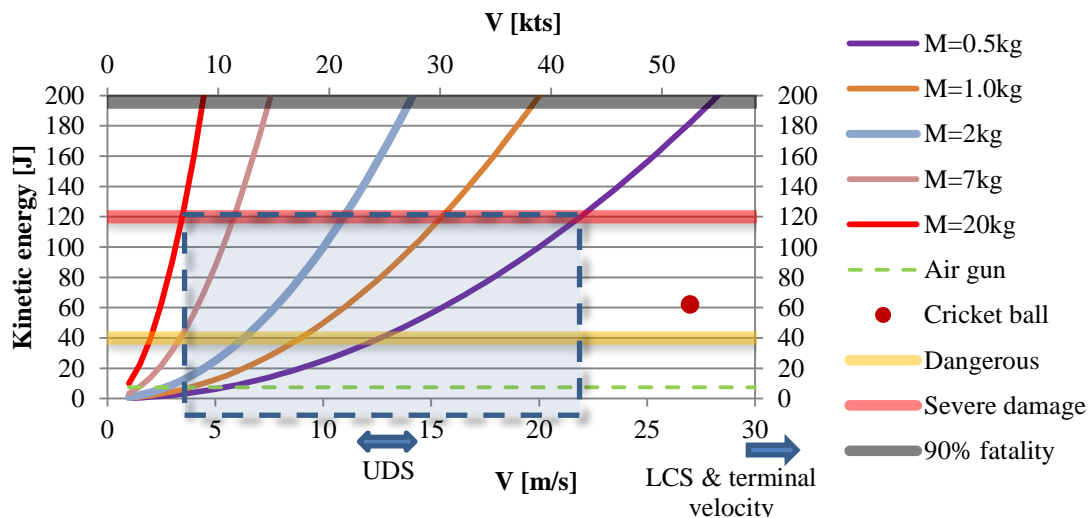


Figure 10: Kinetic energy as a function of RPA mass and velocity. Rough injury estimates are shown as horizontal lines. The present study considers the parameters within the dashed box.

## 7.2 Chest impact

AIS=3 is chosen as the highest acceptable injury severity (AIS=3: serious injury, such as rib fracture or fracture of the sternum). Intuitively, higher RPA mass and velocity increase the injury severity, while a bigger object size reduces the injury severity. Object diameters up to  $D=30\text{cm}$  will be considered, which is approximately the chest width.

Figure 11 shows the model results as combinations of  $M$ ,  $D'$  and  $V$ , which are divided into acceptable and unacceptable regions. To the *left* of each line (which represent a given impact velocity), any combination of  $M$  and  $D'$  results in an injury below AIS=3, which is the acceptable region. To the *right* of each line, the injury severity is unacceptably high. For example, a ten-pin bowling ball ( $M=7\text{kg}$ ,  $D=21\text{cm}$ ) will cause severe injuries if hitting the chest at a velocity of  $7.5\text{m/s}$ , as this mass-velocity combination lies to the right of the  $7.5\text{m/s}$  line. The injuries will be acceptable, if being hit at a velocity of  $5\text{m/s}$ , as this mass-velocity combination lies to the left of the  $5\text{m/s}$  line. These two velocities are equivalent to dropping the ball from heights of  $2.9\text{m}$  and  $1.3\text{m}$ , respectively. The kinetic energies are  $200\text{J}$  and  $87\text{J}$ , respectively (the inflicted deformation energies are lower).

It should be kept in mind, that the limits drawn in Figure 11 are not a life/death distinction. The lines represent serious injury potential with 1per cent probability of death.

When applied to unmanned aircraft: A  $2\text{kg}$  RPA hitting the thorax at  $10\text{m/s}$  ( $20\text{kts}$ ) needs a minimum part diameter of  $15\text{cm}$  to keep the injury potential in the acceptable range. At  $15\text{m/s}$ , an unrealistically large diameter ( $>30\text{cm}$ ) would be required to prevent severe injuries.

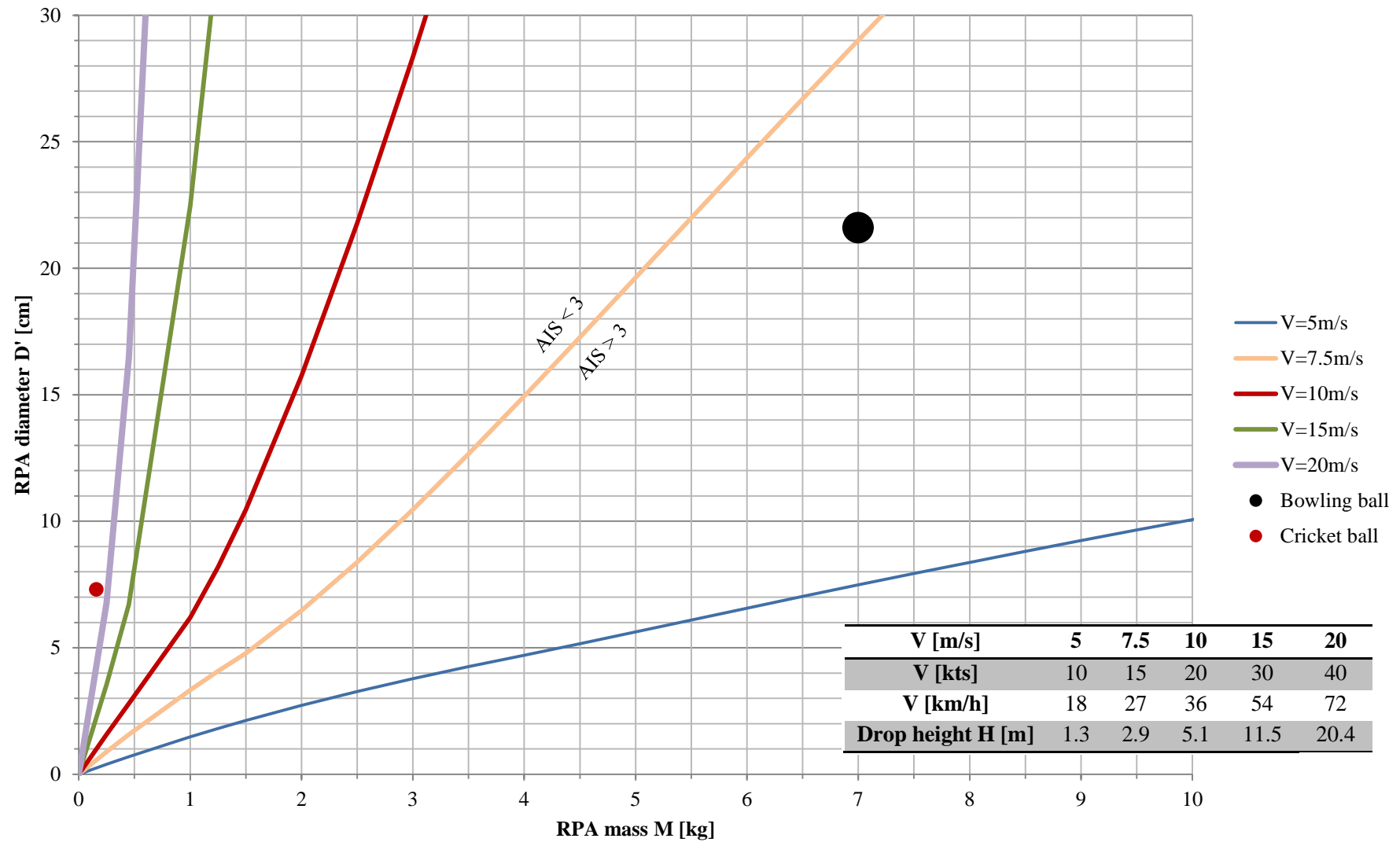


Figure 11: 50% probability of serious injury (AIS=3) of the thorax as a function of RPA impact velocity  $V$ , mass  $M$  and diameter  $D'$ .

### 7.3 Head impact

$BC=1.61$  (representing 50 per cent probability of skull fracture) will be used as the limit for the head injury severity. Figure 12 shows the model results for head impacts: To the left of the solid lines, the injury severity is acceptable, while to the right of the lines skull fracture should be expected for a given impactor size and mass. The dividing lines are steeper than in the thorax impact scenario, implying a higher sensitivity for head injury. For head impacts, the impactor size is not limited to ‘mid-sized’ objects any more, and the limit of an infinite diameter—which is equivalent to a flat surface—needs to be considered. The dashed vertical lines in Figure 12 are such ‘flat plate limits’. They represent the maximum impactor mass for a given velocity that would inflict just the critical injury (50 per cent probability of skull fracture) when the impactor hits the head with its flat side. Any mass higher than this limiting value will lead to head fracture regardless of the contact area / impactor diameter. These limits are equivalent to 76J deformation energy.

A cricket ball will be used for a rough validation of the results for small object impacts. According to the model, a 0.16kg cricket ball becomes dangerous at velocities above 25m/s (100km/h), which is equivalent to  $>50J$ . The lower energy threshold compared to the flat-plate limit is a consequence of the small ball size (small contact diameter  $D$ ). The fastest recorded cricket delivery was 160km/h, with velocities of above 100km/h being the norm. This means that such impacts are very likely to lead to severe or fatal injuries. Table 4 shows that cricket deaths have occurred in the past, but were not directly related to the ball impact. The exception is case 6, where the impact caused an internal haemorrhage; but still no skull fracture was reported. In this case, a rebound of the ball was reported, which reduced the impact energy. This data suggest that the model produces conservative predictions for small object impacts.

	Year	Name	Impact to	Cause of death
1	1870	<a href="#">George Summers</a>	head	abscess in lung
2	1958	<a href="#">Abdul Aziz</a>	chest	heart condition?
3	1971	<a href="#">Roger Davis</a>	head	heart arrest
4	1960s	<a href="#">Nariman Contractor</a>	back head	(survived, retired)
5	1993	<a href="#">Ian Folley</a>	eye	heart attack
6	1998	<a href="#">Raman Lamba</a>	forehead	internal bleeding
7	2009	<a href="#">umpire</a>	head	(not known)

Table 4: Cases of severe or fatal cricket ball injuries (from [Wikipedia](#))

For the large-object limit (the vertical dashed lines), the model predicts 76 Joules as the maximum tolerable deformation energy during an impact with a flat surface. The energy density of the contact area is approximately  $1.6J/cm^2$ . There have been numerous experiments of head impacts on a rigid flat surface, and Table 5 suggests that fractures can be expected for  $E_{def} > 100-200J$ . The critical value of the proposed model is at the lower limit of this range and provides a large margin of safety. On the other hand, the R.C.C. Supplement to standard (321-00, 2000) estimates a 10 per cent probability of fatality (this is similar to an AIS=3 injury) from a 51J impact. Recent computer simulations of head impacts onto flat rigid surfaces show skull fractures only for impact velocities above 6.0-6.5m/s, which is equivalent to 80-95J for a head mass of 4.5kg (Thollon, et al., 2013) (Hamel, et al., 2013). In conclusion, it is reasonable to assume a survivable AIS=3 head injury for deformation energies  $E_{def} < 100J$  in case of a flat surface impact, which is in agreement with the current model.

$E_{def}$	Fracture	Source
37	No	Advani 1975
<b>76</b>	<b>50%</b>	<b>model</b>
104	No	Advani 1975
110	Yes	Allsop 1991
>200	Yes	McIntosh 1993
230	Yes	Stalnaker 1977
260	Yes	Stalnaker 1977

**Table 5: Comparison of the model's maximum tolerable deformation energy during an impact with a rigid flat surface with experimental data.**

A 2kg RPA lies between the solid and dashed lines of  $V=10\text{m/s}$  (20kts). This means that the injury severity is dependent on the diameter contacting the body. While an impact with a flat surface is likely to be tolerable, the contact with any rounded surface is predicted to lead to skull fracture. A lower velocity of  $7.5\text{m/s}$ , on the other hand, is not critical for RPA part diameters above approximately 10cm.

These values should be considered as rough estimates, due to the high sensitivity of the model to the input parameters (such as head diameter  $D_H$  and depression depth  $x_{dep}$ ).

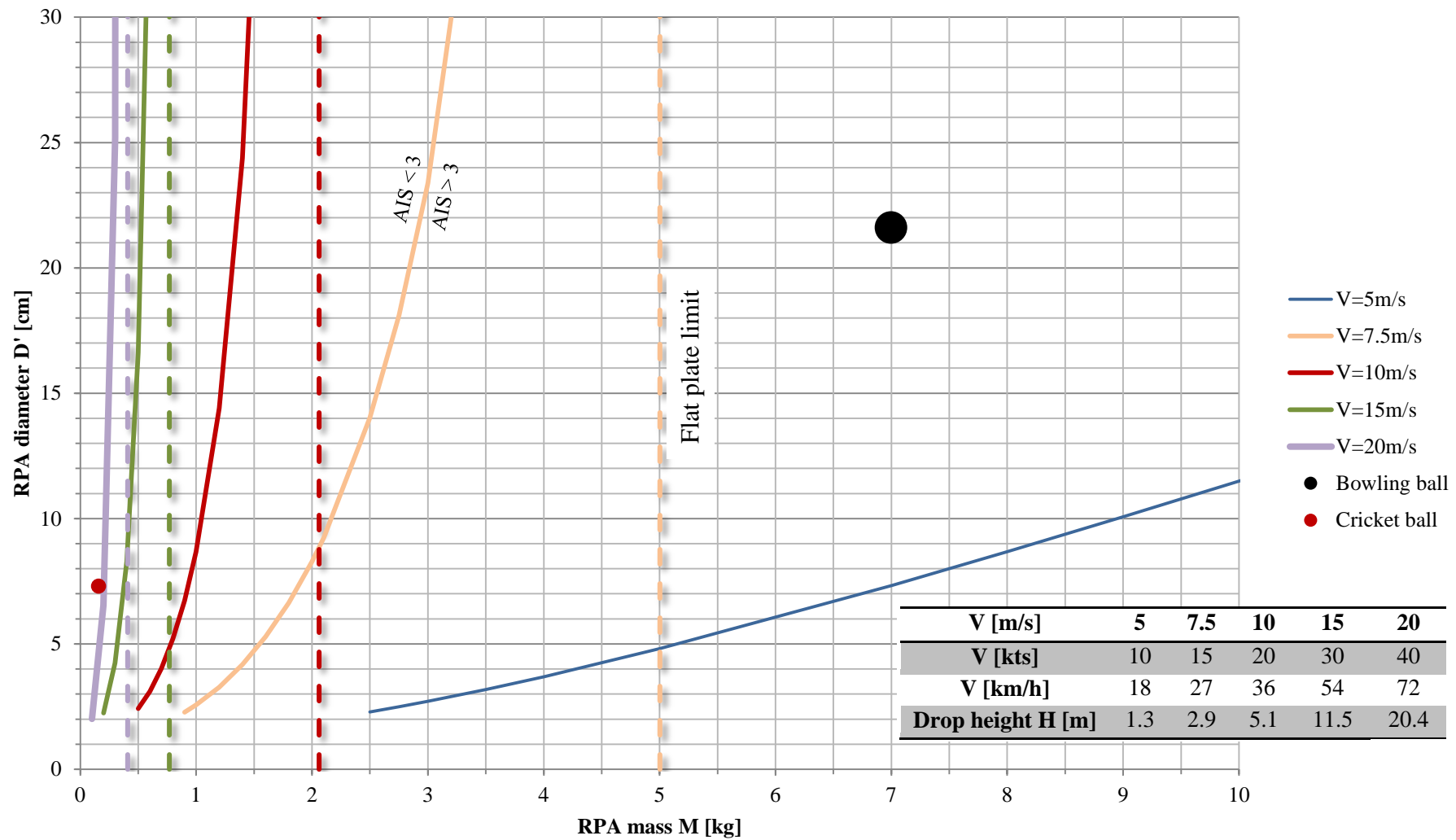


Figure 12: 50% probability of skull fracture as a function of RPA impact velocity  $V$ , mass  $M$  and diameter  $D'$ .

## 8 Discussion of the model

As shown in Figure 13, the proposed injury model has three independent parameters: RPA velocity  $V$  and mass  $M$ , which contribute to the kinetic energy of impact, and the contact diameter  $D$ . The Blunt Criterion requires considering the characteristic diameter of the impacting RPA (or RPA part). This confirms the intuitive assumption that distributing the impact energy over a larger contact area reduces the injury potential. This approach is more reliable for chest injuries and less reliable for head injuries due to the more complex geometry and higher bone stiffness in the latter case. In any case, error bars of up to  $\pm 50\%$  should be applied to the results.

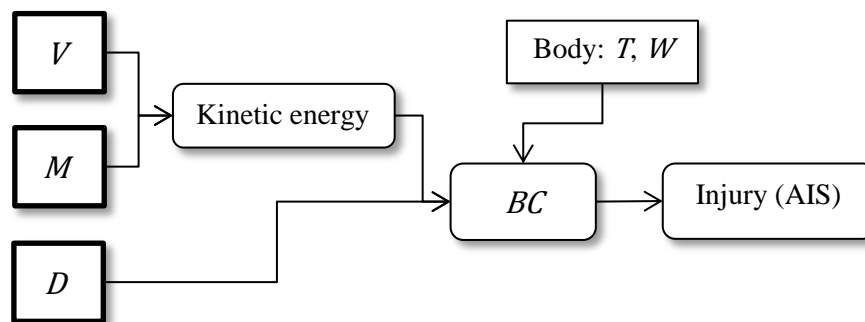


Figure 13: Independent parameters in the proposed model: velocity  $V$ , mass  $M$  and diameter  $D$ .

The model is likely to over-predict the thorax injury severity because the experimental data was obtained from cadaver experiments. (Sturdivan, et al., 2004) observed that dead soft tissue offers less resistance to impact, leading to apparent more severe injuries compared to live specimen.

The skull strength is determined by the thickness of the bone and overlaying soft tissue, which vary across the head surface. The model is based on experiments on the especially vulnerable temporo-parietal region; this is likely to over-predict the injury severity for head impacts.

The modelled victim is from the 5th percentile female population, which biological properties (50kg body mass, thin body wall) make this group most vulnerable. A 75kg male can tolerate more severe chest impacts; but weight and gender were found to not have a significant influence on the head injury tolerance.

The model has the following limitations:

1. The collision dynamics are ignored. The worst case scenario is assumed, in which the RPA impacts with its centre of mass. Any deviation from this scenario leads to lower impact energies.
2. The RPA material stiffness and frangibility are ignored. The current assumption of a rigid body predicts the highest possible deformation energies. Elastic deformations of the contacting RPA surface and/or the destruction of the hull components reduce the blunt injury severity by absorbing a large fraction of the kinetic energy. On the other hand, the creation of hull fragments increases the danger of lacerations and skin penetrating injuries. The regulatory requirement of energy absorbing materials is one possibility to reduce the injury potential.
3. Evidence suggests that chest impacts can be fatal even without leading to substantial physical damage, such as rib fractures (Maron, et al., 1995). Mainly small, fast moving objects (such

as baseballs) can interfere with the natural heart rhythm and lead to cardiac arrests in rare cases. Between 1977 and 1995, 25 fatal baseball chest impacts to youths were recorded in the US (Maron, et al., 1995). This type of injury is not captured by the present model.

4. Secondary injuries to the head and neck from high accelerations (brain concussions, Whiplash) are not captured by the present model. The kinetic energy not used for tissue deformation acts to accelerate the impacted body part (see Figure 2). For example, a 6kg RPA would transfer only 50 per cent of its kinetic energy as deformation energy to the head. The remaining energy would accelerate the head to 50 per cent of the RPA's impact velocity. Assuming an impact duration of 5ms and an impact velocity of  $V=15\text{m/s}$ , this results in an average acceleration of 150G. Under the rigid body assumption, skull fracture is predicted by the current model; yet padding the RPA with energy absorbing materials would increase the chance of high acceleration injuries.
5. The model assumes the free movement of the struck body part. If the movement is restricted, e.g. when hitting the head vertically from above or hitting a lying person, all kinetic energy is transformed into deformation energy. For RPA's lighter than 3kg, this can increase the inflicted energy by up to 30 per cent.
6. Finally, and most importantly, the model is an extrapolation of the Blunt Criterion, which is based on small projectiles (diameter of 2–4cm) and small mass (50–150g) impacting at high velocities ( $>20\text{m/s}$ ). The short impact durations of such low momentum impacts lead to a high energy transfer rate from the projectile to the body, which might result in a different biomechanical response of the body compared to slower but larger impactors (Widder, et al., 1997). No experimental data using the blunt criterion with large impactors were found for an independent validation.

## 9 Conclusions

### 9.1 Summary

1. This study uses AIS=3 as the highest acceptable injury severity, which includes rib fractures or broken sternum for chest impact, and skull fracture for head impacts. The probability of death for this type of injury is less than 10 per cent.
2. The three parameters determining the injury severity are the RPA mass and velocity at impact, and the local radius (diameter) of the RPA part contacting the body.
3. For large impactor diameters (>30cm), the maximum tolerable deformation energies are 120J for the thorax and 76J for the head. The head impact scenario is the limiting case which prescribes the highest acceptable RPA velocity and mass.
4. For a 2kg RPA, the highest tolerable velocity for the head impact is below 7.5m/s (15kts). A minimum RPA part diameter of 10cm is required for this case. The impact energy is equivalent to a solid 11cm aluminium sphere dropped from a height of 3m.
5. A 2kg RPA at 10m/s is predicted to cause skull fracture, even when impacting with its flat side (equivalent to a 2kg aluminium plate dropped from a height of 5m).
6. The results are rough guides only, as the model's input variables show natural variation (e.g. biological parameters) or have been derived from a limited number of experiments. Error bars of  $\pm 50\%$  should be applied.
7. The velocities in the loss-of-control scenario, in which the RPA descends from altitudes >60m reaching its terminal velocity, lie far above the determined acceptable values (typically above 30m/s). At such high impact velocities practically any RPA mass is likely to cause unacceptably severe injuries.

### 9.2 Recommendations

1. The exteriors of small RPA should be designed with as large as possible curvatures (local radius/diameter), within the practical limits of airframe size and aerodynamic considerations.
2. Sharp protrusions should be avoided, particularly beyond the foremost point of the airframe, to prevent skin-penetrating injuries.
3. The use of propeller fairings is recommended. Preference should be given to push propellers.
4. A designed frangibility of the RPA's airframe is recommended to reduce impact loads. Examples are designed weak points, e.g. in the arms of quad copters, or crumple zones on larger RPAs. Crashworthiness research from the automotive industry can provide design guidelines.
5. The following RPA mass and velocities should be regarded as limiting cases that prevent severe injuries:
  - a. **0.4kg at 15m/s (30kts)**
  - b. **1kg at 10m/s (20kts)**
  - c. **2kg at 7.5m/s (15kts)**
6. These limits can be increased significantly by the use of energy absorbing materials for the RPA exterior. Deformable plastics or high density foam reduce the peak forces during impact (think of a soccer ball compared to a hollow aluminium sphere of the same mass & impact velocity).
7. Mitigation measures reducing the impact energy—such as automatically deployed parachutes or automatic descend at minimum velocity—should be employed in a loss-of-control situation.

## 10 APPENDIX

### A. Calculation of the impactor diameter for head impact

Given the depth of the imprint deformation  $x_{def}$  into a soft sphere of diameter  $D_H$  and the effective diameter  $D$ , the associated impactor diameter  $D'$  can be calculated from the intersection of two circles. The relationship between  $D$  and  $D'$  is given by

$$D = \frac{1}{C} \sqrt{\left(-C + \frac{D'}{2} - \frac{D_H}{2}\right)\left(-C - \frac{D'}{2} - \frac{D_H}{2}\right)\left(-C + \frac{D'}{2} + \frac{D_H}{2}\right)\left(C + \frac{D'}{2} + \frac{D_H}{2}\right)}, \quad 15$$

where  $C = \frac{D'}{2} + \frac{D_H}{2} - x_{def}$  is the distance between the sphere centres. This Equation is too complex to analytically determine  $D'$ , and an approximation will be used based on a three-point arc radius as shown in Figure 14. The three points defining the arc are marked by crosses. The middle point is fixed at the distance  $x_{def}$  from the larger sphere's surface, while the outer two points slide along the red lines with the Equation:  $h(D) = \frac{-x_{def}}{D_{FP} - 2T_H}(D - 2T_H) + x_{def}$ . The radius of a three-point arc is:

$$r = \frac{D^2}{8h} + \frac{h}{2} \quad 16$$

Using  $h(D)$  in Equation 16 and setting  $D' = 2r$ , the diameter of the impactor becomes:

$$D' = \frac{D^2}{4x_{def}\left(1 - \frac{D - 2T_H}{D_{FP} - 2T_H}\right)} + x_{def}\left(1 - \frac{D - 2T_H}{D_{FP} - 2T_H}\right) \quad 17$$

The approximation over-predicts  $D'$  by up to 20 per cent for  $D < 20$ cm, which makes it conservative.

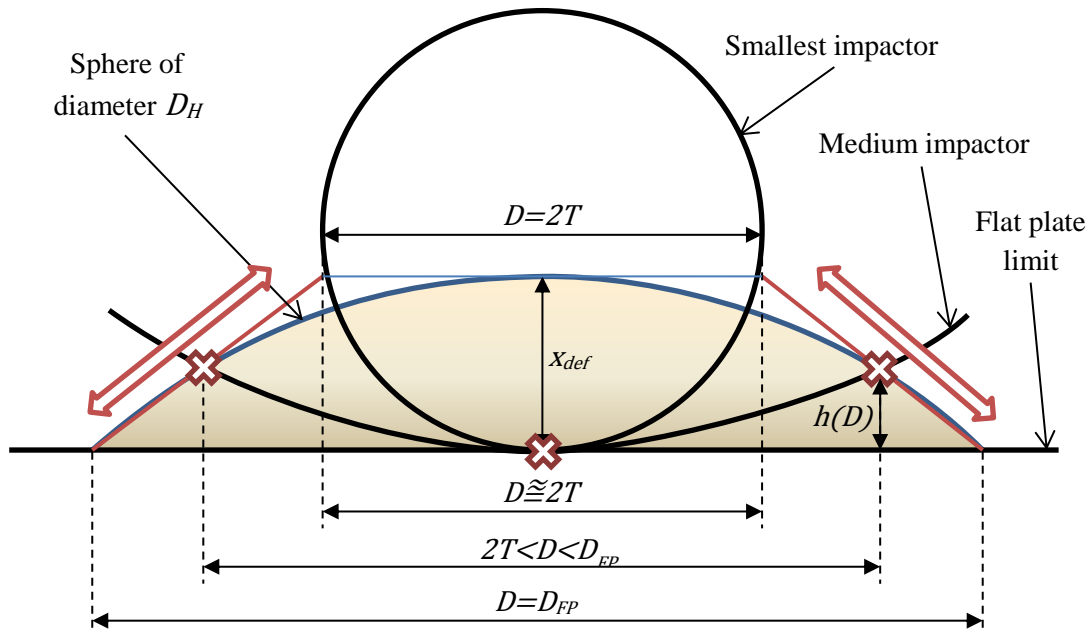


Figure 14: Geometry for calculation of the impactor diameter  $D'$  from a given effective diameter  $D$ .

## B. Cutting injuries by rotating blades

Besides blunt trauma from an RPA impact, the possibility of a cutting injury from the rotating blades needs to be considered. This can be a spinning propeller of a fixed-wing aircraft or the rotating blades of a helicopter-type machine (most commonly a quad copter).

Limited literature could be found only for eye injuries: For blunt impacts by small projectiles (6mm in diameter), (Duma, 2005) compiled experimental data to derive a 50% probability for various eye injury severities. The impact energy thresholds are shown in Table 6.

<b>Injury</b>	<b>Kinetic energy for 50% probability</b>
<b>Corneal abrasion</b>	0.184J
<b>Retinal damage</b>	1.09 J
<b>Globe rupture</b>	4J

**Table 6: Energy thresholds for blunt impact to the eye**

(Alphonse, 2012) performed the only experiments found, in which actual RC (Remotely Controlled) helicopter blades were used on human cadaver eyes. The highest damage severity observed was corneal abrasion. Yet, the experiments are not well documented, and the helicopters used are very light indoor models, with weak motors and light blades. Actual quad-copters in the 1–4lb range should be expected to have a higher damage potential.

## C. 7kg limit justification

It is desirable to define a second – larger – weight limit for large RPA, above the 2kg cut-off. The proposed model does not provide a criterion which would justify any specific weight limit. In particular, an impact with any weight above 2–5kg by far exceeds the defined injury criterion, and is most likely to lead to life threatening injuries.

It is recommended to use a kinetic energy limit, as proposed by (Clothier, et al., 2010). Accepting the fact that high kinetic energy values (>200–500J) are likely to lead to a fatality upon impact, the focus should be shifted from human injury to damage to structures. It is suggested to use penetration of houses by the impacting RPA as damage criterion. This scenario includes (most likely fatal) injuries to people inside the shelter, who are endangered by the remaining kinetic energy of the RPA and debris after structure penetration. The non-penetration of a representative shelter by an impacting RPA is a viable criterion.

The properties of a ‘representative shelter’ depend on the building material, particularly the roof. (Clothier, et al., 2010) state approximately **1400J** as the lower limit for the penetration of a residential home with a corrugated-iron roof. Using this value, the following mass limits are proposed:

- a) 12kg @ 15m/s (30kts)
- b) 7kg @ 20m/s (40kts)
- c) 3kg @ 30m/s (60kts)

## 11 Bibliography

321-00, S. t. s. R., 2000. *Common Risk Criteria for National Test Ranges*, US Army White Sands Missile Range, New Mexico: Secretariat, Range Commanders Council.

Alphonse, V., 2012. *Injury Biomechanics of the Human Eye*, s.l.: Virginia Polytechnic Institute and State University.

Clare, V., J., L., A., M. & Sturdivan, L., 1975. *Blunt trauma data correlation*, s.l.: Edgewood arsenal Aberdeen proving ground.

Clothier, R., Palmer, J., Walker, R. & Fulton, N., 2010. *Definition of airworthiness categories for civil Unmanned Aircraft Systems (UAS)*. Acropolis Conference Centre, Nice, s.n.

Duma, S., 2005. Determination of Significant Parameters for Eye Injury Risk from Projectiles. *The Journal of TRAUMA, Injury, Infection, and Critical Care*, Volume 59, pp. 960-964.

Frank, M., 2012. When backyard fun turns to trauma: risk assessment of blunt ballistic impact trauma due to potato cannons. *International journal of legal medicine*, 126(1), pp. 13-18.

Haddon, D. & Whittaker, C., 2004. *UK-CAA policy for light UAV systems*, s.l.: UK Civil Aviation Authority.

Hamel, A. et al., 2013. Effects of fall conditions and biological variability on the mechanism of skull fractures caused by falls. *International journal of legal medicine*, 127(1), pp. 111-118.

Lim, D., 2005. *Free vibration response of the human head and neck system under normal and mouthguard conditions*. s.l.: Simon Fraser University, Canada.

Magister, T., 2010. The small unmanned aircraft blunt criterion based injury potential estimation. *Safety Science*, Volume 48, p. 1313–1320.

Maron, B., Poliac, L., Kaplan, J. & Mueller, F., 1995. Blunt impact to the chest leading to sudden death from cardiac arrest during sports activities. *New England Journal of Medicine*, 333(6), pp. 337-342.

Raymond, D., Van Ee, C. & Bir, C., 2009. Tolerance of the skull to blunt ballistic temporo-parietal impact. *Journal of Biomechanics*, Volume 42, pp. 2479-2485.

Raymond, D. E., 2008. *Biomechanics of blunt ballistic temporo-parietal head impact*. Wayne State University, Detroit, Michigan: s.n.

Sturdivan, L., Viano, D. & Champion, R., 2004. Analysis of injury criteria to assess chest and abdominal injury risks in blunt and ballistic impacts. *The Journal of TRAUMA, Injury, Infection, and Critical Care*, 56(3), pp. 651-663.

Thollon, L., Llari, M., André, L. & Pascal Adalian, G., 2013. Biomechanical analysis of skull fractures after uncontrolled hanging release. *Forensic Science International*, 233(1), pp. 220-229.

Viano, D., Andrzejak, D., Polley, T. & King, A., 1992. Mechanism of fatal chest injury by baseball impact: development of an experimental model. *Clinical Journal of Sport Medicine*, 2(3), pp. 166-171.

Widder, J., Butz, D. & Milosh, J., 1997. *Assessing the Blunt Trauma Potential of Free Flying Projectiles for Development and Safety Certification of Non-Lethal Kinetic Energy Impactors*, s.l.: Battelle Columbus Operations.

Yoganandan, N. & Pintar, F., 2004. Biomechanics of temporo-parietal skull fracture. *Clinical Biomechanics*, Volume 19, p. 225–239.